JOC Article

Synthesis, Structure, and Computational Studies of Soluble Conjugated Multidentate Macrocycles

Amanda J. Gallant, Joseph K.-H. Hui, Federico E. Zahariev, Yan Alexander Wang,* and Mark J. MacLachlan*

University of British Columbia, Department of Chemistry, 2036 Main Mall, Vancouver BC V6T 1Z1, Canada

mmaclach@chem.ubc.ca; yawang@chem.ubc.ca

Received April 13, 2005

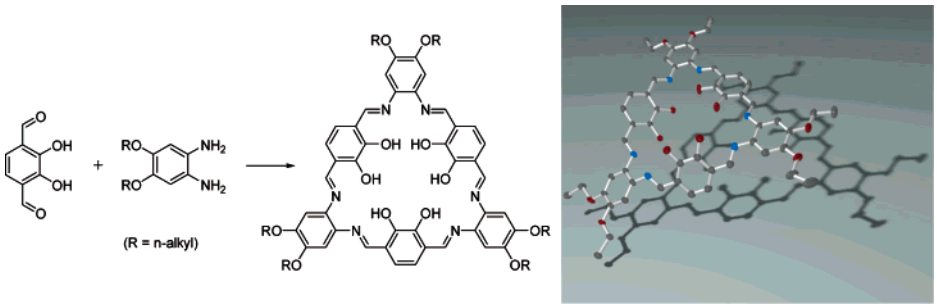

Conjugated, shape-persistent macrocycles based on [3 + 3] Schiff-base condensation are of interest for supramolecular materials. In an effort to develop new discotic liquid crystals based on these compounds, a series of macrocycles with peripheral alkoxy groups of varying length have been prepared. The synthesis and mechanism of formation have been probed by isolation of oligomeric intermediates. A single-crystal X-ray diffraction study of one macrocycle revealed a nonplanar, strongly hydrogen-bonded structure. To our surprise, even with very long substituents, the macrocycles were not liquid crystalline. This has been rationalized by ab initio calculations that indicate the macrocycles are undergoing rotation of the dihydroxydiiminobenzene rings that may not allow a stable discotic liquid crystalline phase. These results provide new insight into the formation and properties of these large macrocycles and may provide guidance to developing stable liquid crystalline materials in the future.

Introduction

Macrocycles have played a pivotal role in the development of supramolecular chemistry.[1] In particular, macrocycles capable of coordinating to metals and ions, such as crown ethers,[2] cryptands,[3] and cyclodextrins,[4] are important for the investigation of supramolecular interactions.[5] These substances have also been used for various applications, such as nanoreaction chambers,[6] solubilizing agents for membrane transport,[7] phase-transfer reagents,[8] and in the development of chemical sensors.[9]

Rigid macrocycles of nanoscopic dimensions may serve as the basis for creating new porous materials.[10,11] Metal-containing macrocycles that are assembled by metal−ligand interactions, and depend on them for the stability of the final product, are well-known.[12−14] On the other

(1) (a) Lehn, J.-M. *Acc. Chem. Res.* **1978**, *11*, 49−57. (b) Hof, F.; Craig, S. L.; Nuckolls, C.; Rebek, J., Jr. *Angew. Chem., Int. Ed.* **2002**, *41*, 1488−1508. (c) Bong, D. T.; Clark, T. D.; Granja, J. R.; Ghadiri, M. R. *Angew. Chem., Int. Ed.* **2001**, *40*, 988−1011. (d) Cronin, L. *Annu. Rep. Prog. Chem., Sect. A* **2004**, *100*, 323−383. (e) Gale, P. A. *Philos. Trans. R. Soc. London A* **2000**, *358*, 431−453. (f) Atwood, J. L.; Barbour, L. J.; Hardie, M. J.; Raston, C. L. *Coord. Chem. Rev.* **2001**, *222*, 3−32.

(2) (a) Gokel, G. W.; Leevy, W. M.; Weber, M. E. *Chem. Rev.* **2004**, *104*, 2723−2750. (b) van Veggel, F. C. J. M.; Verboom, W.; Reinhoudt, D. N. *Chem. Rev.* **1994**, *94*, 279−299.

(3) (a) Sarkar, B.; Mukhopadhyay, P.; Bharadwaj, P. K. *Coord. Chem. Rev.* **2003**, *236*, 1−13. (b) Zhang, X. X.; Izatt, R. M.; Bradshaw, J. S.; Krakowiak, K. E. *Coord. Chem. Rev.* **1998**, *174*, 179−189. (c) Albrecht, M.; Röttele, H.; Burger, P. *Chem. Eur. J.* **1996**, *2*, 1264−1268.

(4) (a) Harada, A. *Acc. Chem. Res.* **2001**, *34*, 456−464. (b) Rizzarelli, E.; Vecchio, G. *Coord. Chem. Rev.* **1999**, *188*, 343−364. (c) Jiang, Y.; Zhang, H.; Li, H.; Wu, M.; Zhang, S.; Wang, J. *J. Mol. Struct.* **2004**, *702*, 33−37.

(5) (a) Lehn, J.-M.; Ball, P. *New Chem.* **2000**, 300−351. (b) Atwood, J. L.; Barbour, L. J.; Dalgarno, S.; Raston, C. L.; Webb, H. R. *J. Chem. Soc., Dalton Trans.* **2002**, 4351−4356. (c) Nelissen, H. F. M.; Kercher, M.; De Cola, L.; Feiters, M. C.; Nolte, R. J. M. *Chem. Eur. J.* **2002**, *8*, 5407−5414.

(6) Kim, H.-J.; Heo, J.; Jeon, W. S.; Lee, E.; Kim, J.; Sakamoto, S.; Yamaguchi, K.; Kim, K. *Angew. Chem., Int. Ed.* **2001**, *40*, 1526−1529.

10.1021/jo050742g CCC: $30.25 © 2005 American Chemical Society
Published on Web 08/26/2005

CHART 1. Phenyleneethynylene and Schiff-Base Macrocycles

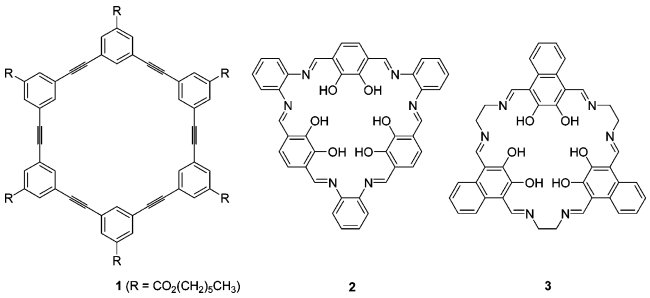

hand, large rigid organic macrocycles containing only covalent bonds are still few in number.[10,15] These are exemplified by phenyleneethynylene macrocycles (e.g., **1**), which have been studied for their ability to organize into assemblies (Chart 1).[10,11b] Moreover, these macrocycles may form the basis of tubular liquid crystals.[16]

We identified rigid, conjugated macrocycles that could bind multiple transition metals as useful targets. These compounds may function as ligands for the development of new size- and shape-selective catalysts or for developing new coordination materials. Most routes to large organic macrocycles involve many steps, templation, or high dilution and are not easily scaled up. However, Schiff-base chemistry offers an excellent route to synthesizing large, covalently bonded structures. The reaction is reversible, allowing the controlled preparation of thermodynamically stable products. Numerous researchers have used Schiff-base condensation as the ring-closing step to synthesize macrocycles, often in high yield.[17−19]

With the goal of developing conjugated macrocycles that could coordinate to multiple metals and be easily prepared, we identified macrocycle **2** as an attractive target. Preliminary studies of a related macrocycle **3** prepared using a Ba^{2+} template were reported by Reinhoudt et al.[20] Akine et al. prepared macrocycle **2** in a two week synthesis and studied its structure by X-ray crystallography.[21] Unfortunately, these macrocycles are nearly insoluble in organic solvents (e.g., $CHCl_3$, MeOH, and MeCN). Soluble analogues of such macrocycles should exhibit interesting electrochemical, photochemical, and sensing properties. In 2003, we reported a synthesis for soluble, conjugated macrocycle **6e** and demonstrated that it assembles into novel supramolecular architectures upon coordination with small cations.[22]

Conjugated macrocycle **2** is anti-aromatic, possessing 48 π-electrons. Anti-aromatic compounds possessing 4n π-electrons in a conjugated ring (e.g., cyclobutadiene) are generally unstable or highly reactive. They typically undergo distortions from planarity to break the conjugation and render the molecule more stable; for example, cyclooctatetraene has a boat conformation. In the case of macrocycle **1**, which also possesses 48 π-electrons, the molecule is not anti-aromatic since the conjugation is broken by the *m*-phenylene linkages. Thus, this molecule is flat since any other conformation would invoke strain. However, in the case of macrocycle **2**, twisting is a possible mechanism to break conjugation without strain.

Here, we report our studies on the synthesis, characterization, and computations of soluble conjugated Schiff-base macrocycles, as well as the isolation of some fragments and byproducts that give insight into the mechanism of macrocycle formation. We also report the structure of a conjugated macrocycle that is organized in a tubular arrangement in the crystalline state.

Discussion

Synthesis and Characterization. The condensation of aldehydes with amines is a route to imines, functional

(7) Visser, H. C.; Reinhoudt, D. N.; de Jong, F. *Chem. Soc. Rev.* **1994**, *23*, 75−81.

(8) (a) Shirakawa, S.; Yamamoto, K.; Kitamura, M.; Ooi, T.; Maruoka, K. An*gew. Chem., Int. Ed.* **2005**, *44*, 625−628. (b) Häger, M.; Holmberg, K. *Chem. Eur. J.* **2004**, *10*, 5460−5466.

(9) (a) Beer, P. D.; Gale, P. A. *Angew. Chem., Int. Ed.* **2001**, *40*, 486−516. (b) Kim, J.; McQuade, D. T.; McHugh, S. K.; Swager, T. M. *Angew. Chem., Int. Ed.* **2000**, *39*, 3868−3872. (c) Morey, J.; Orell, M.; Barceló, M. À.; Deyà, P. M.; Costa, A.; Ballester, P. *Tetrahedron Lett.* **2004**, *45*, 1261−1265. (d) Trippé, G.; Levillain, E.; Le Derf, F.; Gorgues, A.; Sallé, M.; Jeppesen, J. O.; Nielsen, K.; Becher, J. *Org. Lett*. **2002**, *4*, 2461−2464.

(10) (a) Staab, H. A.; Neunhoeffer, K. *Synthesis* **1972**, 424. (b) Zhao, D.; Moore, J. S. *Chem. Commun.* **2003**, 807−818. (c) Höger, S. *Chem. Eur. J.* **2004**, *10*, 1320−1329. (d) Bunz, U. H. F.; Rubin, Y.; Tobe, Y. *Chem. Soc. Rev*. **1999**, *28*, 107−119.

(11) (a) Müller, P.; Usón, I.; Hensel, V.; Schlüter, A. D.; Sheldrick, G. M. *Helv. Chim. Acta* **2001**, *84*, 778−784. (b) Henze, O.; Lentz, D.; Schlüter, A. D. *Chem. Eur. J.* **2000**, *6*, 2362−2367. (c) Campbell, K.; Kuehl, C. J.; Ferguson, M. J.; Stang, P. J.; Tykwinski, R. R. *J. Am. Chem. Soc.* **2002**, *124*, 7266−7267.

(12) (a) Leininger, S.; Olenyuk, B.; Stang, P. J. *Chem. Rev.* **2000**, *100*, 853−908. (b) Fujita, M. *Chem. Soc. Rev*. **1998**, *27*, 417−425.

(13) For recent examples of coordination macrocycles, see: (a) Mukherjee, P. S.; Das, N.; Kryschenko, Y. K.; Arif, A. M.; Stang, P. J. *J. Am. Chem. Soc.* **2004**, *126*, 2464−2473. (b) Sun, S.-S.; Stern, C. L.; Nguyen, S. T.; Hupp, J. T. *J. Am. Chem. Soc.* **2004**, *126*, 6314−6326. (c) Jiang, H.; Lin, W. *J. Am. Chem. Soc.* **2004**, *126*, 7426−7427.

(14) (a) Takahashi, R.; Kobuke, Y. *J. Am. Chem. Soc.* **2003**, *125*, 2372−2373. (b) Beer, P. D.; Berry, N. G.; Cowley, A. R.; Hayes, E. J.; Oates, E. C.; Wong, W. W. H. *Chem. Commun.* **2003**, 2408−2409. (c) Eisenberg, A. H.; Ovchinnikov, M. V.; Mirkin, C. A. *J. Am. Chem. Soc.* **2003**, *125*, 2836−2837. (d) Newkome, G. R.; Cho, T. J.; Moorefield, C. N.; Mohapatra, P. P.; Godínez, L. A. *Chem. Eur. J.* **2004**, *10*, 1493−1500.

(15) (a) Grave, C.; Schlüter, A. D. *Eur. J. Org. Chem.* **2002**, 3075−3098. (b) Yamaguchi, Y.; Yoshida, Z.-I. *Chem. Eur. J.* **2003**, *9*, 5430−5440. (c) Ma, C.; Lo, A.; Abdolmaleki, A.; MacLachlan, M. J. *Org. Lett.* **2004**, *6*, 3841−3844. (d) Baxter, P. N. W. *Chem. Eur. J.* **2003**, *9*, 5011−5022. (e) Campbell, K.; McDonald, R.; Tykwinski, R. R. *J. Org. Chem.* **2002**, *67*, 1133−1140. (f) Grave, C.; Lentz, D.; Schäfer, A.; Samori, P.; Rabe, J. P.; Franke, P.; Schlüter, A. D. *J. Am. Chem. Soc.* **2003**, *125*, 6907−6918. (g) Yuan, L.; Feng, W.; Yamato, K.; Sanford, A. R.; Xu, D.; Guo, H.; Gong, B. *J. Am. Chem. Soc.* **2004**, *126*, 11120−11121.

(16) (a) Fischer, M.; Lieser, G.; Rapp, A.; Schnell, I.; Mamdouh, W.; De Feyter, S.; De Schryver, F. C.; Höger, S. *J. Am. Chem. Soc.* **2004**, *126*, 214−222. (b) Höger, S.; Enkelmann, V.; Bonrad, K.; Tschierske, C. *Angew. Chem., Int. Ed*. **2000**, *39*, 2268−2270. (c) Mindyuk, O. Y.; Stetzer, M. R.; Heiney, P. A.; Nelson, J. C.; Moore, J. S. *Adv. Mater.* **1998**, *10*, 1363−1366. (d) Sessler, J. L.; Callaway, W.; Dudek, S. P.; Date, R. W.; Lynch, V.; Bruce, D. W. *Chem. Commun*. **2003**, 2422−2423.

(17) Vigato, P. A.; Tamburini, S. *Coord. Chem. Rev.* **2004**, *248*, 1717−2128.

(18) (a) Akine, S.; Hashimoto, D.; Saiki, T.; Nabeshima, T. *Tetrahedron Lett.* **2004**, *45*, 4225−4227. (b) Shimakoshi, H.; Kai, T.; Aritome, I.; Hisaeda, Y. *Tetrahedron Lett.* **2002**, *43*, 8261−8264. (c) Gawroński, J.; Kołbon, H.; Kwit, M.; Katrusiak, A. *J. Org. Chem.* **2000**, *65*, 5768−5773. (d) Zhao, D.; Moore, J. S. *J. Org. Chem.* **2002**, *67*, 3548−3554.

(19) (a) Beckmann, U.; Brooker, S. *Coord. Chem. Rev.* **2003**, *245*, 17−29. (b) Veauthier, J. M.; Cho, W.-S.; Lynch, V. M.; Sessler, J. L. *Inorg. Chem.* **2004**, *43*, 1220−1228. (c) Givaja, G.; Blake, A. J.; Wilson, C.; Schröder, M.; Love, J. B. *Chem. Commun.* **2003**, 2508−2509. (d) Gao, J.; Reibenspies, J. H.; Martell, A. E. *Angew. Chem., Int. Ed.* **2003**, *42*, 6008−6012.

(20) Huck, W. T. S.; van Veggel, F. C. J. M.; Reinhoudt, D. N. *Recl. Trav. Chim. Pays-Bas* **1995**, *114*, 273−276.

(21) Akine, S.; Taniguchi, T.; Nabeshima, T. *Tetrahedron Lett*. **2001**, *42*, 8861−8864.

(22) Gallant, A. J.; MacLachlan, M. J. *Angew. Chem., Int. Ed.* **2003**, *42*, 5307−5310.

SCHEME 1. Synthesis of Soluble Conjugated Macrocycles 6a−l

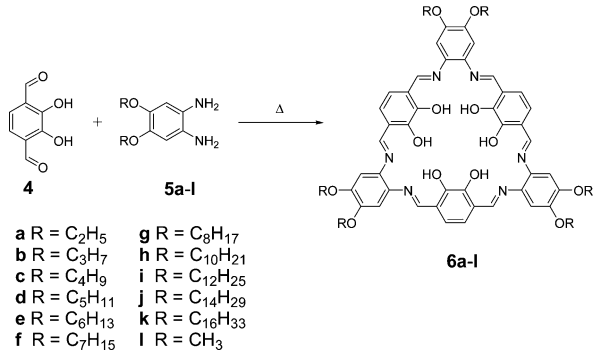

groups with carbon−nitrogen double bonds. By increasing the functionality of the precursors, one can obtain polymers, oligomers, or macrocycles. We have developed a convenient procedure to synthesize conjugated Schiff-base macrocycles **6a**−**k**, with peripheral alkoxy groups, Scheme 1. To modify the solubility of the macrocycles, dialkoxyphenylenediamine precursors **5a**−**k** with alkyl chains of varying length have been employed. Macrocycle **6l** with methoxy substituents could not be purified due to its insolubility.

The reaction of diol **4** with diamines **5** afforded red, fibrous or microcrystalline products **6** in moderate to high yield (typically 50−80% for **6a**−**h**; lower for longer chains). Mass spectra (ESI-MS) of the macrocycles all show the expected protonated products and Na^+ complexes. In addition, peaks corresponding to $[\mathbf{6}_2 + Na]^+$ and $[\mathbf{6}_3 + Na_2]^{2+}$ were often observed. These arise from ion-induced aggregation of the macrocycles in solution.[22] The IR spectra for **6a**−**k** confirm single imine functionality with a C=N stretch (1610 cm^{-1}) and show no aldehyde C=O absorption from starting material **4** (1660 cm^{-1}). The ^1H NMR spectra of **6a**−**k** (Figure 1) are consistent with the expected D_{3h} symmetry of the macrocycle with one imine (δ = 8.5 ppm) and two singlet aromatic resonances (δ = 6.6, 6.9 ppm). On the basis of 2D NMR experiments (HMQC, HMBC), the aromatic resonances are assigned to protons situated on the catechol portion of the macrocycle (6.9 ppm) and on the phenylenediamine portion (6.6 ppm). These are each shifted from the resonances observed for starting materials **4** and **5** found at 7.23 and 6.36 ppm, respectively. The phenolic OH resonance is observed at 13.3 ppm, where the significant downfield shift arises from strong hydrogen-bonding to the nearby imine. The ^{13}C NMR spectra of **6a**−**k** are also consistent for a macrocyclic structure with a single imine resonance found between 161 and 163 ppm.

It is noteworthy that the reaction between compound **4** and phenylenediamines with shorter substituents (e.g., **5a**−**f**) proceed much more rapidly than the reaction with longer diamines (e.g., **5g**−**k**). Whereas the reaction to form macrocycle **6e** typically requires only 1−3 h, the reaction to form macrocycle **6k** requires 12+ h to go to completion. This difference in reactivity may be due to aggregation of the phenylenediamines in the reaction solvent (1:1 $CHCl_3$/MeCN).

The macrocycles appear to bind strongly to small molecules, such as small cations (e.g., NH_4^+, Na^+)[22] and water. ^1H NMR spectra of the macrocycles show broad water resonances between 1.9 and 2.5 ppm in $CDCl_3$. The significant downfield shift from 1.5 ppm, the usual chemical shift of water in $CDCl_3$, is indicative of hydrogen bonding. These results suggest that macrocycles **6** may form supramolecular complexes with small, polar molecules, and this is currently under investigation.

These compounds are intensely colored, analogous to porphyrins and phthalocyanines, but are not luminescent. In the solid state, they appear deep red to brown in color and they absorb very strongly in the UV−vis region of the spectrum with peaks centerd at ca. 400 nm ($\epsilon \sim 8 \times 10^4$ mol L^{-1} cm^{-1}), as shown in Figure 1. This intense transition is primarily attributed to the $\pi-\pi^*$ transition of the conjugated ring.

Crystals of macrocycle **6a** were obtained from DMF, and the single-crystal X-ray diffraction (Figure 2) confirms that the structure is a macrocycle. Moreover, the macrocycle is nonplanar, as in the case of the related structure reported by Akine.[21] The molecule is triangular in shape, with the apexes defined by the three diethyloxyphenylenediimine moieties. There are six hydroxyl groups within the molecule that are strongly hydrogen bonded to the adjacent imines, with average intramolecular O···N distances of 2.60(4) Å. Two sides of the macrocycle are twisted along the C−N···N−*C* axis[23] such that the catechol groups are twisted out of the plane of the macrocycle in opposite directions. The third side[23] is nearly planar, with the catechol group only twisted slightly out of the plane. Intermolecular π-stacking is apparent between the flat sides of the macrocycles in the solid-state, with nearest intermolecular separations of 3.59 Å along the stacking axis. The macrocycles are arranged in layers and stacked in a way that reveals a porous structure when viewed normal to the (100) axis, as shown in Figure 2c (the pores contain DMF solvent molecules). Other examples of porous crystalline structures based on shape-persistent macrocycles are known.[11]

Self-Assembly. The macrocycle synthesis is remarkably efficient, and the [3 + 3] macrocycle is the major product obtained. As the preparation of macrocycles **6a**−**k** depends on the assembly of six different components (three of the diformyl species, **4**, and three phenylenediamine species, **5**), it likely occurs stepwise through several intermediates. The previously published report of macrocycle **2** indicated observations of a 2:2 condensation product, formed from the reaction of two diformyl moieties and two phenylenediamine molecules, as well as a postulated oligomeric compound composed of three molecules of each of the starting materials but where ring-closing condensation has not occurred.[21] Although these are sensible intermediates of the condensation process, we have not observed either of these intermediates during our studies of related macrocycles possessing alkoxy substituents (**6**).

We were, however, able to isolate other small fragments of these macrocycles through variation of the reaction conditions. The difficulty encountered trying to isolate the fragments is that they tend to decompose or condense to afford macrocycles during attempts to purify

(23) From the crystallographic data found in the Supporting Information, the two sides of the macrocycle twisted along the C−N···N−*C* axis are more specifically C20−N4···N5−C29 and C34−N6···N1−C1, and the third side that is nearly planar can be defined by C6−N2···N3−C15.

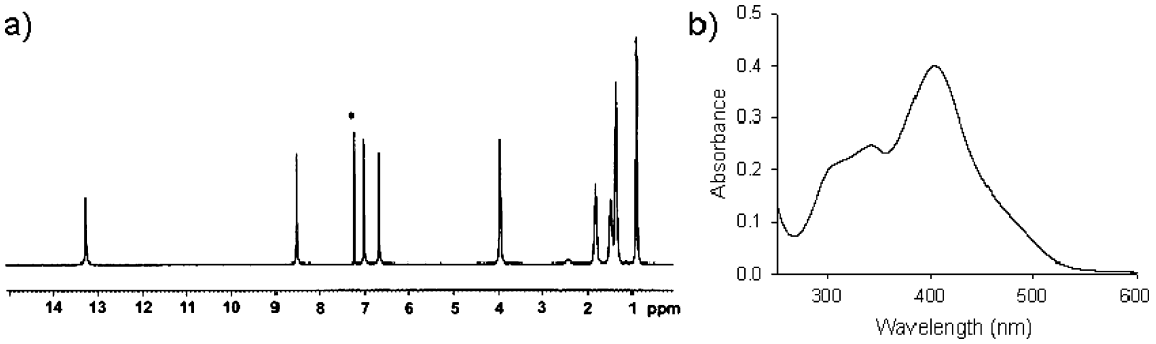

FIGURE 1. (a) ^{1}H NMR spectrum (300 MHz, $CDCl_3$) of **6e**; (b) UV−vis spectrum of **6e** (ca. 4.0×10^{-6} M in CH_2Cl_2).

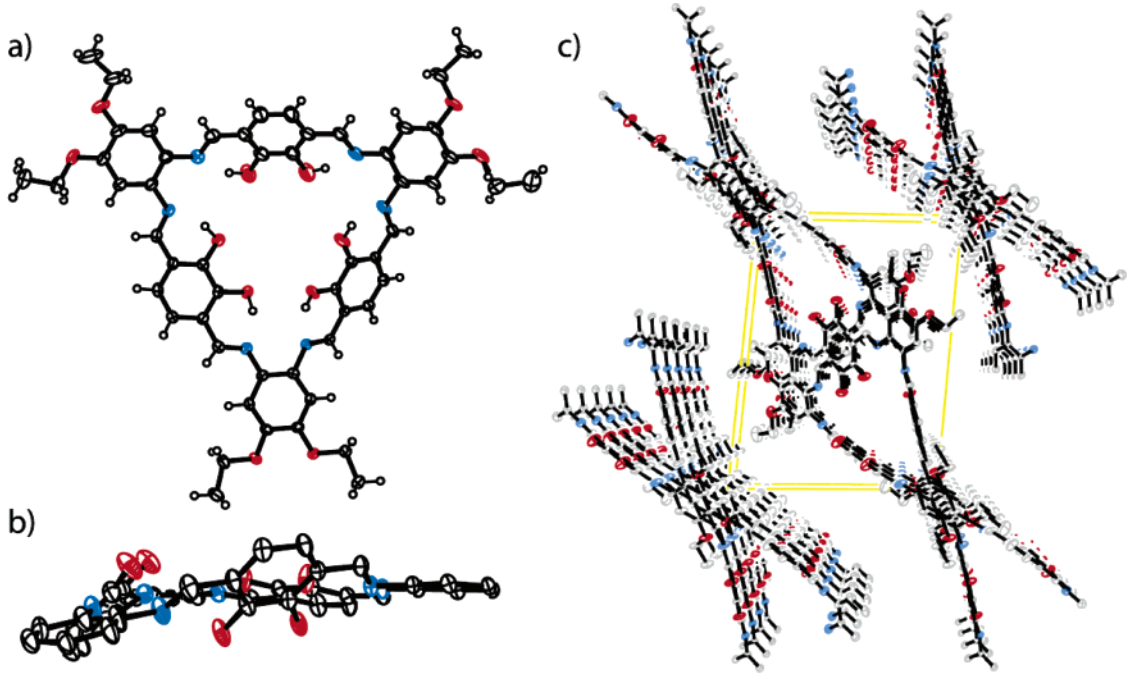

FIGURE 2. Molecular structure of macrocycle **6a** as determined by single-crystal X-ray diffraction with thermal ellipsoids at 50% probability. Solvent molecules are removed for clarity. Red = oxygen, blue = nitrogen. (a) View from the top of the macrocycle showing strong intramolecular hydrogen bonding. (b) View of macrocycle **6a** from the side showing the nonplanarity of the macrocycle (ethyloxy groups and hydrogen atoms are removed for clarity). (c) View of the packing diagram for macrocycle **6a** normal to the (100) axis, revealing the stacking pattern forming pores.

them by recrystallization or column chromatography. Thus, it has been necessary to find conditions where the fragments are obtained in the highest possible purity directly from the reaction. When using longer alkoxy chains (10 or more carbon atoms) and keeping the reaction temperature between 0 and 25 °C, the major product observed is the 1:1 condensation product **7**.[24] The ^{1}H NMR spectrum of **7j** (R = $C_{14}H_{29}$, prepared using **5j**) shows both a formyl and an imine peak (9.93 and 8.54 ppm, respectively) with the two phenolic protons shifted downfield due to hydrogen-bonding with the imine nitrogen and the formyl group (13.70 and 10.90 ppm, respectively).[24] Most distinctive is the aromatic region of the spectrum with two doublets for the phenolic ring and two singlets for the diaminobenzene ring. The IR spectrum for compound **7j** is similar to that of macrocycles **6** with the addition of an aldehyde C=O stretch at 1686 cm^{-1} and amine N−H stretches at 3390 and 3315 cm^{-1}. The UV−vis spectrum of this compound contains three major peaks (304, 338, and 413 nm) and a broad shoulder (~460 nm) with an overall shape quite different from that for macrocycles **6**.

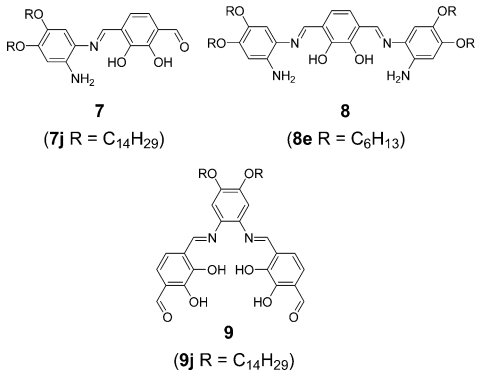

(24) Gallant, A. J.; Patrick, B. O.; MacLachlan, M. J. *J. Org. Chem.* **2004**, *69*, 8739−8744.

SCHEME 2. Reaction of Intermediates To Form Macrocycle 6

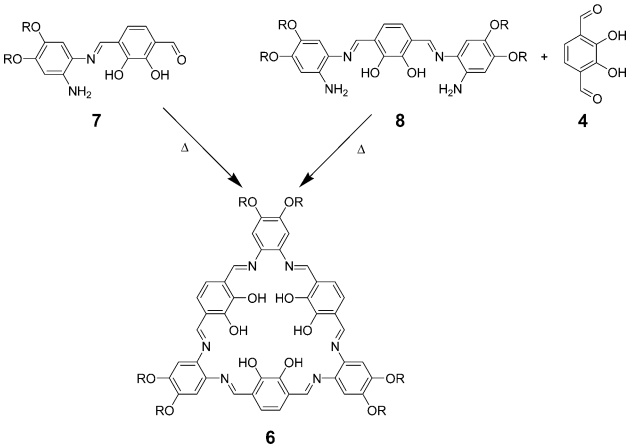

By performing this condensation reaction at room temperature and adjusting the stoichiometry appropriately a 1:2 condensation product (**8**) is obtained. The ESI-MS indicates that when diamine **5e** was employed, pure product **8e** was obtained, and the ^{1}H NMR spectrum shows three singlets in the aromatic region rather than the two observed for the macrocycle. The IR spectrum shows both a C=N (1611 cm^{-1}) stretch and N−H stretches (3376, 3303, 3169 cm^{-1}), with no evidence of any aldehyde C=O stretches. The UV−vis spectrum of **8e** is similar to that of **7j** at lower wavelengths (306 and 346 nm) but is red shifted at higher wavelengths (468 nm) and different from that of macrocycle **6**.

To prove that compounds **7** and **8** are intermediate species in macrocycle formation, both were shown independently to form macrocycle **6** (Scheme 2). Compound **7j** was heated in $CHCl_3$ forming macrocycle **6j** as the major product (ca. 70% by ^{1}H NMR), with a mixture of byproducts including compound **10**. When compound **8e** was heated in $CHCl_3$ with 1 equiv of **4**, macrocycle **6e** was produced (ca. 90% by ^{1}H NMR). The fact that **8** reacts in the presence of **4** to give macrocycle **6** indicates that the reaction conditions allow for the hydrolysis of an imine bond in **8**.

Compound **9**, formed by the reaction of diamine **5** with 2 equiv of compound **4**, is an intermediate that might be expected to form during the condensation. This species, however, has proven very difficult to isolate. Only through reaction of excess diol **4** (4−5 equiv) with diamine **5j** were we able to obtain this product (with an impurity of **4**), as verified by ESI-MS. The ^{1}H NMR spectrum shows resonances attributed to an aldehyde, an imine, and three aromatic protons (two doublets and a singlet). In addition, the OCH_2 groups appear as a well-defined triplet, indicative of a symmetrical environment for the phenylenediamine moiety.

The isolation of compounds **7**−**9** in the reactions of **4** with **5** suggests that the macrocycles are assembled stepwise. Small oligomers form and eventually reach the correct length to cyclize into the [3 + 3] macrocycle. These isolated oligomeric compounds are also of interest as precursors to preparing unsymmetrically substituted macrocycles that incorporate two different phenylenediamine molecules. Such macrocycles may be assembled if the rates of condensation and hydrolysis of the imines are significantly different, or if the hydrolysis of the fragments is prevented by chelation to a metal. This may enable preparation of amphiphilic macrocycles for assembly in Langmuir−Blodgett films or of alkanethiol-functionalized macrocycles for assembly on gold surfaces.

It is noteworthy that the [3 + 3] condensation product is the only species isolated without any observation of larger macrocycles or oligomers. Macrocycles **6** could be prepared in $CHCl_3$, $CHCl_3$/MeCN, or toluene, indicating that the solvent is likely not templating the macrocycle formation. Akine et al. proposed that the driving force for the formation of **2** was the insolubility of the macrocycle.[21] To prove that this is not the case for macrocycles **6** with alkoxy substituents, compounds **4** and **5e** were reacted in $CHCl_3$ under dilute enough conditions that the product did not precipitate. Upon rapid solvent removal, ^{1}H NMR spectroscopy of the mixture indicated that macrocycle **6e** was the major species in solution. In the case of macrocycle **2**, crystallization may indeed be a driving force since the product is much less soluble than macrocycles **6** and crystallizes more easily.

In theory, the condensation of compounds **4** and **5** in a 1:1 ratio could form a [3 + 3] macrocycle, larger macrocycles, or linear (helical) oligomers and polymers. We believe that the obtained [3 + 3] macrocycle is thermodynamically favored as it minimizes strain and maximizes intramolecular hydrogen bonding. Experimentally, the [3 + 3] macrocycle is a strongly favored product and remains the major product even when trying to hinder macrocycle formation by the addition of a full equivalent of salicylaldehyde as a capping species to the preparation. Also, no evidence for tautomerism has been observed in any of the macrocycles **6a**−**k** or the fragments **7**−**9**.

Reactivity. The reactivity of the macrocycle itself is difficult to probe due to the presence of many functional groups (ether, imine, alcohol), but intermediates and byproducts in the condensation can provide insight into its reactivity. Phenylenediamines are known to undergo various reactions with benzaldehyde, including reactions to form benzimidazoles and benzimidazolines.[25] In the formation of macrocycles **6**, the reaction generally proceeds smoothly to the final product. This is quite surprising since a wide variety of side reactions is possible.

We have observed that under certain conditions (50 °C, acid catalyst) the major product in the synthesis of macrocycle **6e** is not the fully conjugated macrocycle, but instead monoreduced macrocycle **10e**.[24] In addition, this compound can often be isolated as a minor byproduct in the synthesis of **6e**. We have proposed that monoreduced macrocycle **10e** is formed by the reduction of macrocycle **6e** with a benzimidazoline intermediate generated in situ from the 1:1 condensation product **7** producing a highly fluorescent benzimidazole.[24] In our previous report, we observed benzimidazole in the reaction mixture by ESI-MS and were able to isolate and characterize a small quantity of the benzimidazole **11e**. Formation of benzimidazoline is a likely process during the reaction. Thus, monoreduction of the macrocycle may be favored to break the anti-aromaticity of the ring.

During our attempts to prepare **9** with hexyloxy substituents (i.e., **9e**), a byproduct was isolated in low yield. The MS of the new product shows the expected

(25) Smith, J. G.; Ho, I. *Tetrahedron Lett.* **1971**, 3541−3544.

mass for a 2:1 diol/diamine species (i.e., **9e**), but the ^{1}H NMR spectrum shows two aldehyde groups, two OCH_2 groups, no imine, and several aromatic peaks. The characterization data are consistent with benzimidazole **12**. Compound **12** may be derived from the 2:1 condensation product **9**, through a cyclization followed by simultaneous oxidation and reduction. Alternatively, the oxidation/reduction process may occur stepwise.[24] It is noteworthy that the reaction of benzaldehyde with phenylenediamine leads to the formation of benzimidazoles without isolation of the diimine. In our case, the hydroxyl groups stabilize the imine and reduce its tendency to cyclize.

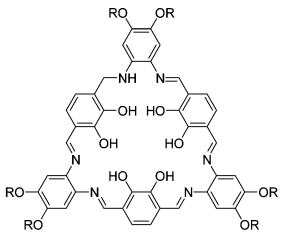

10

(**10e** R = C_6H_{13})

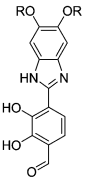

11

(**11e** R = C_6H_{13})

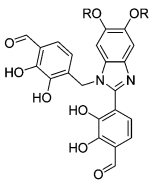

12

(**12e** R = C_6H_{13})

Liquid Crystallinity. Since the macrocycles, as drawn in Scheme 1, appear to possess D_{3h} symmetry similar to triphenylene mesogens, we anticipated that they would form discotic liquid crystals. Macrocycles with long alkoxy chains (e.g., **6g**−**k**) were prepared and investigated by differential scanning calorimetry (DSC) and polarizing optical microscopy (POM). Melting transitions were observed for **6g**−**k**, but no transition to a liquid crystalline phase was detected by either DSC or POM.

The addition of different groups (e.g., poly(alkoxy)-benzene derivatives) to the periphery of the macrocycles may be necessary to further suppress the melting points and yield liquid crystalline phases. On the other hand, our inability to observe liquid crystallinity in macrocycles **6a**−**k** may be linked to the ring structure of the core. Macrocycle **1** and triphenylenes are both planar and readily form discotic liquid crystalline phases. Macrocycle **6**, which is anti-aromatic, may distort in a way that breaks the symmetry in the molecule and inhibits the generation of a liquid crystalline phase.

Calculations. The experimental NMR spectra of the macrocycles **6** show an average symmetry that corresponds to a planar macrocycle (D_{3h} symmetry) in solution. A low-temperature ^{1}H NMR experiment indicated that this symmetry is retained to below −85 °C. In the solid-state, however, the macrocycles appear to have a distortion in which the catechol moieties are all oriented out of the plane. To obtain a better understanding of their conformations and dynamics, we have undertaken a computational study of the macrocycles. As a model, ab initio computations were performed on macrocycle **6l** with peripheral methoxy substituents. Geometry optimizations and frequency calculations were performed in B3LYP/6-31G(d,p), after a preliminary geometry optimization in HFS/STO-3G and B3LYP/4-31G. UV−vis spectra were computed in CIS(D), TD, and ZINDO. No symmetry constraints were applied unless indicated.

Preliminary calculations starting with a near-planar conformation indicated that the macrocycle has two stable conformations, neither of which is flat (Figure 3). In the first conformation (**A**), the molecule has approximately C_s symmetry, with the phenylenediimine groups coplanar and all of the catechol moieties oriented out of the plane, but with two up and one down.[26] The other conformation (**B**) has C_{3v} symmetry and lies only 1.6 kcal/mol above the C_s isomer. Again, the OH groups of the catechol moieties are oriented out of the plane, but are all on the same side of the macrocycle. The planar configuration (D_{3h} symmetry) of the macrocycle (forced with constraints) has an energy that is ca. 14.4 kcal/mol above the C_s isomer **A**.

The absence of planarity in the macrocycle for conformations **A** and **B** is consistent with the solid-state structure obtained for **6a**. It is not surprising that this macrocycle would be nonplanar, since it is anti-aromatic, possessing 48 electrons in the closed π-system of the large macrocycle. As a result of this anti-aromaticity, the macrocycle adopts a nonplanar conformation that retains the planarity and aromaticity of the substituted benzene components that make up the macrocycle.

In solution, the macrocycles appear to have D_{3h} symmetry, indicating that the calculated structures must interconvert on the NMR time scale. The macrocycle has three easy rotation axes passing through the catechol moieties between imine carbon atoms, Figure 4. One possibility for interconversion between isomers **A** and **B** is via the rotation of one catechol group while the others remain stationary. To evaluate the energy profile for such a rotation, we performed a relaxed rotation calculation using DFT. Starting with the C_{3v} isomer **B**, a catechol moiety was rotated about one of the easy axes of rotation shown in Figure 4. The dihedral angles of the two Ph−N bonds (i.e., C−C−N=C) along the same side of the triangle were fixed in 10° intervals, and the structure was permitted to relax to the nearest local minimum energy for each position with this constraint. Figure 5 shows the relative calculated energy for the minimized structures as a function of dihedral angle. Most notably, there are four local minima, including two that we had not encountered before. The rotation scan revealed two local minima in which one catechol is directed away from the center of the macrocycle. Figure 3 shows the macrocycle in each of these two new conformations (**C** and **D**).

Overall, the calculated values of the bond lengths and angles for the conformations agree well with those deduced from the X-ray diffraction study of macrocycle **6a**. Table 1 provides a comparison of the bond lengths measured and computed for the macrocycles. Typically, the bond lengths are within 0.1 Å.

For the macrocycles to interconvert between the local energy minima, they must surmount a barrier of only

(26) In every stable conformation of the macrocycle, the phenylenediimine rings are coplanar, and we refer to these as the "plane of the macrocycle", recognizing that the macrocycle is not truly planar.

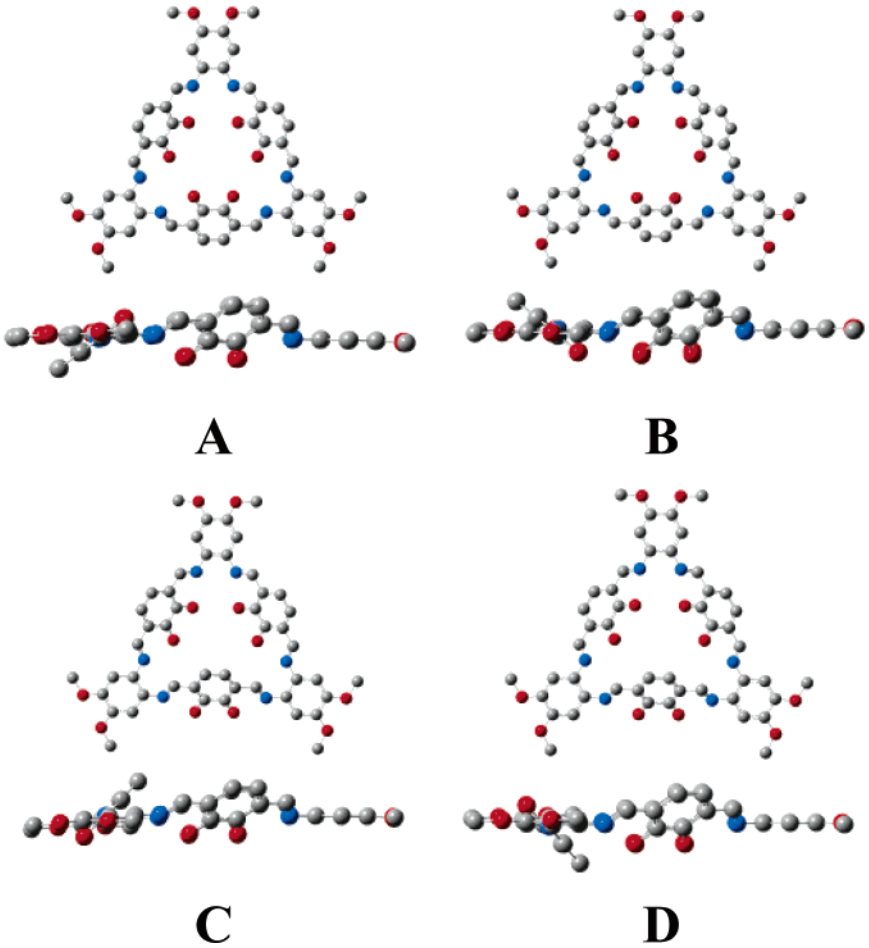

FIGURE 3. Computed low energy conformations **A**−**D** for macrocycle **6l**. Views of the structures are shown from the top and side of the macrocycle, with hydrogen atoms omitted for clarity.

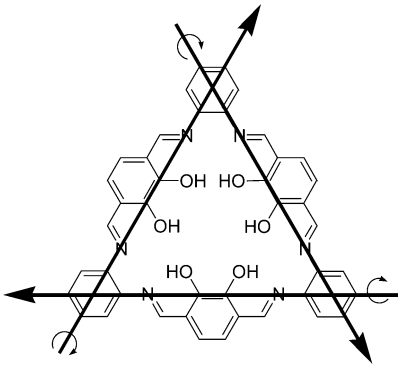

FIGURE 4. Three easy rotation axes for macrocycle **2**.

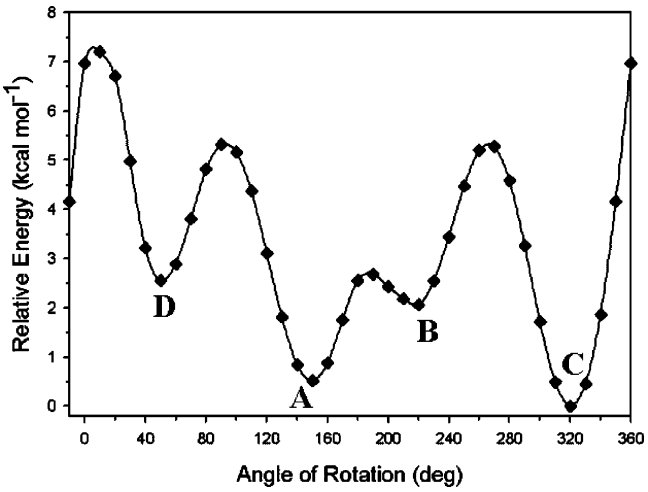

FIGURE 5. Relaxed scan of rotation computed for macrocycle **6l**. The angle of rotation corresponds to the dihedral angle of the C−C−N=C bond. A dihedral angle of 0° indicates that the catechol undergoing rotation in 10° intervals is oriented toward the center of the macrocycle; for a dihedral angle of 180°, the catechol is oriented away from the center of the macrocycle.

ca. 5 kcal/mol. At room temperature, the conformations may readily interconvert without actually passing through a flat conformation. Any catechol moiety may move to the other side of the macrocycle either by allowing the hydroxyl groups to pass through the center of the ring, or alternatively to rotate outside of the ring (i.e., the aromatic protons moving through the center). The latter motion, where the hydroxyl groups rotate outside of the center of the macrocycle, has a lower energy barrier. These calculations are consistent with our observation that the conformations cannot be "frozen out" at −85 °C. Although the macrocycles appear in solution to have D_{3h} symmetry, they are in fact rapidly interconverting between the local energy minima and never have D_{3h} symmetry.

TABLE 1. Comparison of Selected Bond Lengths and Angles for the Macrocycles

bond	measured for **6a** (SCXRD)	computed for **6l** (conformation **A**)	computed for **6l** (conformation **C**)	computed for **6l** (D_{3h} conformation)
C−N (Å)	1.415(6)	1.403	1.400	1.408
C=N (Å)	1.284(6)	1.294	1.295	1.300
C−OH (Å)	1.354(4)	1.334	1.336	1.327
HOC=COH (Å)	1.402(4)	1.424	1.422	1.424
C−CN (Å)	1.454(8)	1.448	1.449	1.446
HO−C−COH (deg)	117.7(4)	117.4	117.4	117.4
C=N−C (deg)	121(1)	121.6	122.3	122.7
N−C−CCOH (deg)	122(1)	122.0	122.3	123.0

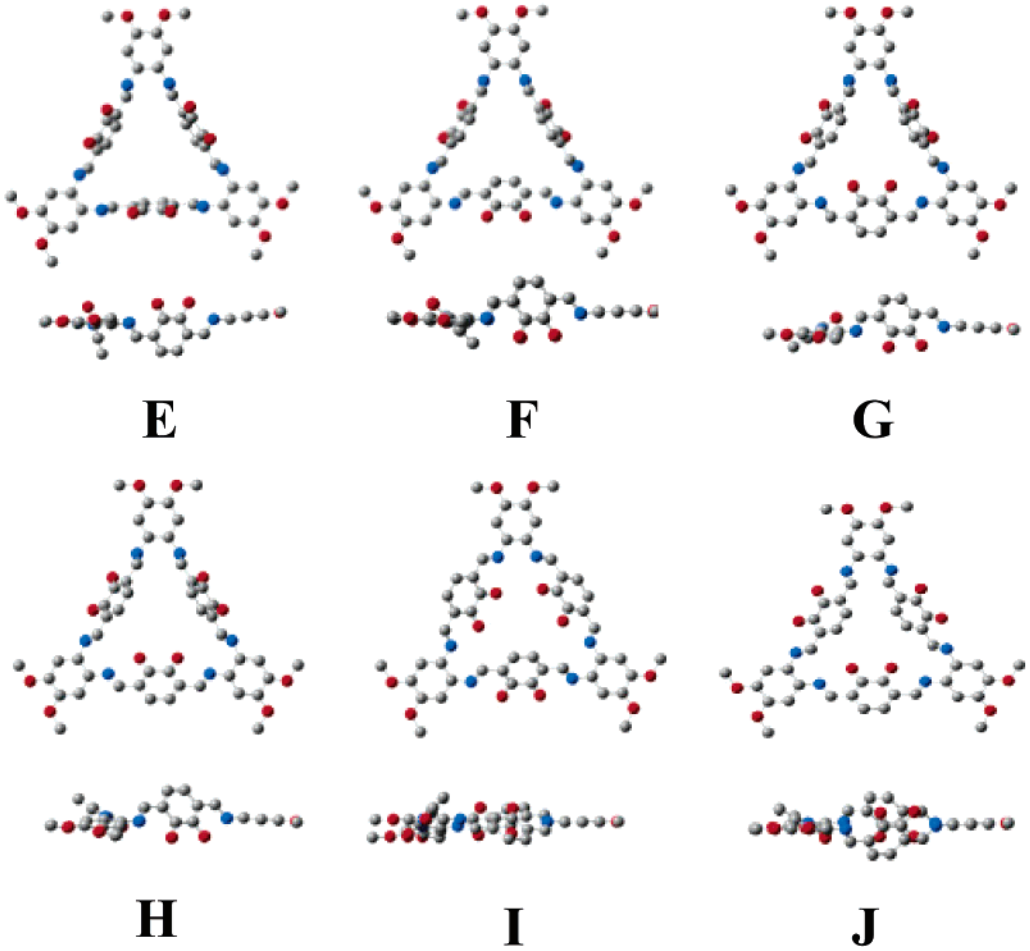

FIGURE 6. Computed low energy conformations **E**−**J** for macrocycle **6l**. Views of the structures are shown from the top and side of the macrocycle, with hydrogen atoms omitted for clarity.

After discovering that the lowest energy conformations of the macrocycle may involve the orientation of the hydroxyl moieties away from the center of the ring, we searched for local minima starting with conformations where one, two, or three of the catechol moieties are oriented with their hydroxyl groups away from the center of the ring. We started with different possible orientations of the catechols (e.g., one with all of the catechol moieties oriented up and away from the center of the ring) and allowed the system to relax without constraints. Six new local minima were identified, and the respective conformations are illustrated in Figure 6.

All of the conformations are higher in energy than conformation **C**. The conformation where two catechols are oriented away from the center (one up, one down) with the third oriented toward the center (**I**) is closely related to conformation **D** and is only slightly higher in energy than conformation **C**. Conformation **E**, in which all three catechols are oriented with the hydroxyl groups oriented slightly away from center, but on the same side of the macrocycle, has C_{3v} symmetry and is much higher in energy than conformation **C**. Conformation **F** is similar to conformation **C**, but with one of the catechol moieties rotated by ∼180°. This leads to a high energy conformation (9.9 kcal/mol above **C**). Table 2 summarizes the energies and symmetries of all of the conformations observed.

The computed structure **C** is not necessarily the global minimum structure. We have not searched for all possible conformations of the macrocycle. We have searched enough possibilities, though, to suggest that this is likely close in energy and geometry to the global minimum.

TABLE 2. Calculated Energies of the Conformations A–J for Macrocycle 6l Relative to Conformation C

conform.	energy[a]	approximate symmetry	conform.	energy[a]	approximate symmetry
A	0.5	C_s	**F**	9.9	C_s
B	2.1	C_{3v}	**G**	8.9	C_s
C	0.0	C_s	**H**	6.3	C_s
D	2.6	C_s	**I**	0.4	C_1
E	17.2	C_{3v}	**J**	2.3	C_1

[a] kcal/mol.

TABLE 3. Measured and Calculated Values for the ^{13}C and ^{1}H NMR Chemical Shifts of Selected Atoms

atom	measured[a] (ppm)	measured[b] (ppm)	calcd[c] (ppm)	calcd[d] (ppm)	calcd[e] (ppm)
C=N	161	165	176.1	156.5	151.6
C–OH	151	151	163.7	150.5	151.1
C–C=N	121	120	125.6	117.6	116.6
C–H (catechol)	121	121	125.0	115.9	115.5
C–N	135	143	151.2	141.0	137.9
H–O	13.2	13.5	13.9	13.4	13.7
H–C (OH ring)	7.0	7.3	7.2	6.8	8.0
H–C=N	8.5	9.1	9.2	8.5	9.2

[a] Measured from macrocycle **6e** in $CDCl_3$. [b] Measured from **2** in DMF-d_7 (ref 21). [c] Computed for conformation **A** of macrocycle **2** in HF/6-311+G(2d,p). [d] Computed for conformation **A** of macrocycle **2** in b3lyp/6-31g(d,p). [e] Computed for the flat conformation of macrocycle **2** in b3lyp/6-31g(d,p). All values are relative to TMS.

In the crystalline state, the conformation of macrocycle **6a** most closely resembles the calculated structure **A** with approximately C_s symmetry. This agrees with our calculations that this conformation should be a stable conformation. The influences of crystal packing, intermolecular interactions (e.g., π-stacking), and solvent likely affect the relative stability of this conformation over the calculated minimum of conformation **C**.

Properties. Properties (NMR, IR, UV–vis) of the macrocycle were computed for comparison with experimental values and to evaluate the computed models of the macrocycle. ^{1}H and ^{13}C NMR chemical shifts were calculated on the flattened structure (D_{3h}) and conformations **A**–**I** of macrocycle **2** without alkoxy substituents using two methods with different basis sets. The macrocycle without alkoxy substituents was selected as it offers a close resemblance to the macrocycles of interest with the benefit of reduced computational demand. Calculated and measured ^{13}C and ^{1}H NMR chemical shifts of selected atoms in the macrocycle are tabulated in Table 3.

The computed NMR chemical shifts are in reasonably good agreement with the measured values. As well, the chemical shifts for the different conformations analyzed are quite consistent with one another, particularly for the ^{13}C shifts. It is clear that the B3LYP method with a smaller basis set gave better agreement with the experimental values than HF methods with a large basis set. Differences between the calculated and measured values may be a result of solvent interactions, particularly in the case of hydrogen-bonding atoms, and the truncation of the peripheral alkoxy substituents to protons. Moreover, the real molecule is sampling a variety of conformations, not just the fixed conformations assumed for the purpose of the NMR calculation.

To examine the electronic properties of the conjugated macrocycle, the semiempirical ZINDO method was employed. Starting with the geometry-optimized flat conformation of macrocycle **2**, the electron densities of the ground state and the first excited state were computed. Figure 7 shows the pictures of the highest occupied molecular orbital (HOMO) and lowest unoccupied molecular orbital (LUMO); each of these is doubly degenerate. The lowest energy excitation from the ZINDO calculation is mostly HOMO to LUMO in nature, but there is additional mixing of other transitions. The calculated UV–visible spectrum for **2** shows a maximum at ca. 405 nm. This is in close agreement with the experimental spectra, Figure 1, which have maxima at ca. 402–404 nm for macrocycles **6**.

The electron density difference between the ground state and the first excited state was computed, Figure 8. This arises from the difference between the HOMO and the LUMO. Notably, the arrangement of the π-electrons in the aromatic structure changes significantly. From a chemical standpoint, the ground state has a benzenoid structure, while the first excited state has a quinoidal structure, which is a high-energy resonance structure for the macrocycle. This is illustrated in Figure 9.

IR and Raman spectra of the macrocycles were also computed using B3LYP/6-31G(d,p). Overall, the calculated IR spectrum for **2** was similar to the experimental spectra of the macrocycles. An intense peak calculated at ca. 1622 cm^{-1} corresponds to a vibration that is mostly C=N stretching (coupled with significant O–H and C–H stretching). This agrees well with the measured C=N stretching mode of ~1610 cm^{-1} for macrocycles **6**.

Macrocycle Twisting. In all of the minimized conformations, a characteristic dihedral twist along the Ph-N bond is observed. It seems the nature of the dihedral twist is dictated by π-electron delocalization rather than electrostatic effects of repulsion between hydroxyl groups. *N*-Methyleneaniline was chosen as a representative fragment of the macrocycle for calculation. It is surprising that a similar twist could be found even in this simple model compound depicted in Figure 10.

The nonplanarity of the macrocycle might be due in part to the anti-aromatic character of the macrocycle, but there is another significant component as deduced by computation. The dihedral angle between the imine and benzene ring (C–C–N=C) in *N*-methyleneaniline (Figure 10) is 38°. A detailed electronic structure analysis has been performed on conformations of stilbene-like species, (4-X-Ph)–CH=N–Ar (Ar = 2-pyridyl, X = –Cl, –NO_2, –$N(Me)_2$; Ar = 2-pyrimidyl, X = –NO_2).[27] Using a novel fragmented molecular orbital basis set method, the authors concluded that the driving force for the out-of-plane twist in systems of this type is the interplay between the σ-orbital interaction and the quantum mechanical resonance energy of the π-system, which is destabilizing in this case. It is likely that similar interactions are responsible for the nonplanarity of the conjugated macrocycles in this study. However, we cannot rule out the possibility that repulsive interactions of the hydroxyl groups in the interior of the macrocycle and steric interactions between the imine H and C–H of the phenylenediimine contribute to the destabilization of the flat conformation of the macrocycle.

(27) Yu, Z.-H.; Li, L.-T.; Fu, W.; Li, L.-P. *J. Phys. Chem. A* **1998**, *102*, 2016–2028.

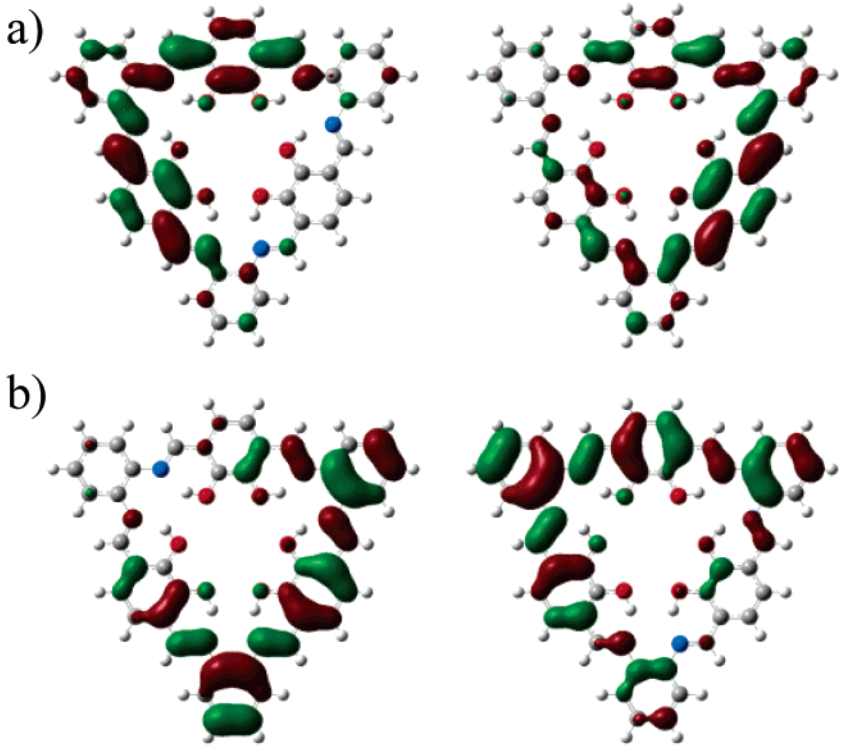

FIGURE 7. (a) Degenerate LUMOs of macrocycle **2** in the flat conformation (D_{3h}) calculated by ZINDO. (b) Degenerate HOMOs of macrocycle **2** in the flat conformation calculated by ZINDO.

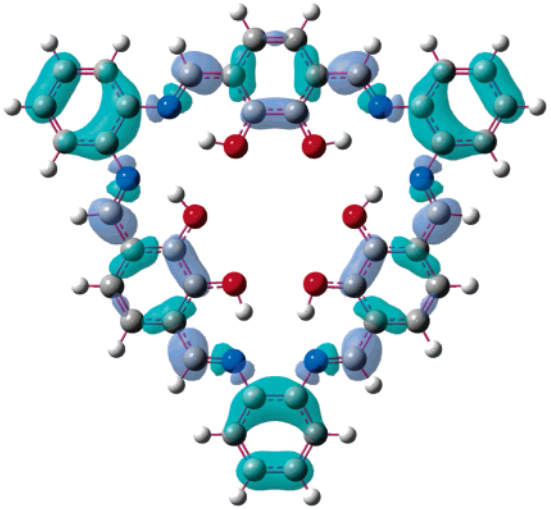

FIGURE 8. Difference electron density map between the ground state and first excited state of flattened macrocycle **2** as determined by ZINDO.

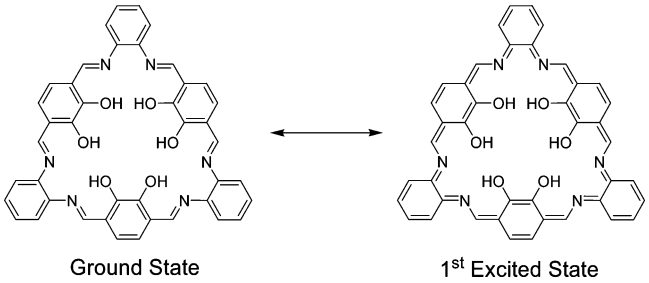

FIGURE 9. Ground state and first excited state of the flattened macrocycles may be represented as resonance structures of one another.

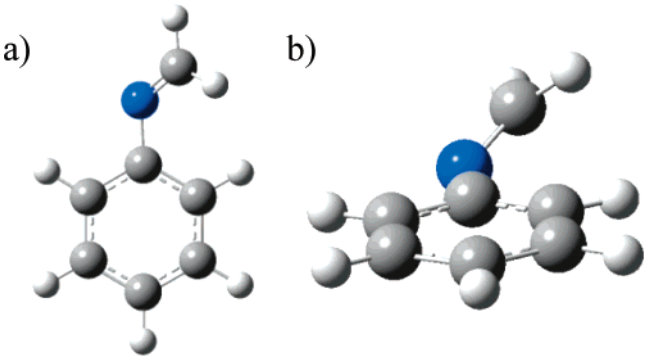

FIGURE 10. Dihedral twisting in *N*-methyleneaniline shown from the top (a) and side (b). The dihedral angle $D_{(C-C-N=C)}$ is about 38°. This model compound represents a small component of the macrocycle.

Summary

We have described the convenient synthesis and characterization of disc-shaped, soluble macrocycles possessing peripheral alkoxy chains. The macrocycles are formed from the Schiff-base condensation of a substituted phenylenediamine with 1,2-dihydroxy-3,6-diformylbenzene. Several oligomeric intermediates in the reaction, including 1:1, 2:1, and 1:2 condensation products, have been isolated, providing evidence that the macrocycles are formed in a stepwise manner. Moreover, a single-crystal X-ray diffraction study of **6a** indicated that the macrocycle was nonplanar and organized into a tubular structure in the solid state. Density functional theory has been used to compute the properties of the macrocycles and to understand the interconversion of the various confor-

mations available to the macrocycle. These macrocycles are promising candidates for developing new supramolecular structures and for multinuclear coordination chemistry.

Acknowledgment. We thank Jonathan Chong and Brian Patrick for solving the structure of compound **6a**, Britta Boden for low-temperature NMR experiments on **6e**, and Dr. Yun Ling for helpful discussions. We acknowledge Westgrid for computational support. We are grateful to the University of British Columbia and the Natural Sciences and Engineering Research Council of Canada (NSERC) for funding and for graduate scholarships to A.J.G.

Supporting Information Available: Experimental details, NMR spectra for new compounds, atomic coordinates from computational studies, and X-ray crystallographic data (CIF). This material is available free of charge via the Internet at http://pubs.acs.org.

JO050742G